Radiation Hardness and Mechanical Durability of Kuraray Optical Fibers

K. Hara, K. Hata, S. Kim, M. Mishina*, M. Sano, Y. Seiya, K. Takikawa, M. Tanaka, and K. Yasuoka

Institute of Physics, University of Tsukuba, Tsukuba-shi, Ibaraki-ken 305, Japan

Fermi National Accerelator Laboratory, Batavia, Illinois 60510, USA

Abstract:

The radiation hardness of Kuraray 3HF scintillating and clear optical fibers has been investigated using ^{60}Co γ-rays in the dose range from 0.4 krad to 500 krad. Significant initial degradation in the attenuation length was observed both for 3HF and clear fibers at a dose as small as 10 krad. The radiation hardness of both the scintillating and clear fibers is identical if it is expressed in terms of the ratio of the attenuation lengths after to before irradiation. The radiation damage of 3HF fibers was observed to recover substantially with a time scale of a few months. The attenuation length and mechanical durability against bending were measured for clear fibers by changing S parameter which characterizes the softness of the fibers.

PACS numbers: 29.40.−n, 42.81.Bm, 42.88.+h

(Submitted to NIM A on September 24, 1997)

1. Introduction

Plastic scintillating and clear optical fibers have become one of the key detector elements in high energy experiments such as in fiber tracking systems and tile-fiber calorimeters. Radiation hardness remains to be an important issue for systems that have to be operated in high radiation environment. Ref. 1 reports that the attenuation length of plastic fibers is shortened to about 60% of the original value after irradiation of 100 krad. Their measurement covers the dose range 100 krad and above. We have carried out a series of radiation tests of Kuraray 3HF scintillating fibers and clear fibers to investigate the radiation hardness at smaller doses, extending the dose coverage down to ~0.4 krad.

The attenuation length and mechanical durability against bending are also important parameters. This is of particular important for clear fibers of the tracker system where long clear fibers extract scintillating signals out of the detector complex through limited space. Kuraray has developed softer and more flexible fibers (S type) than the original type (or non-S type) fibers for their applications to tile-fiber calorimeters where the wavelength-shifting fibers are bent at a radius of a few cm and embedded in scintillator plates [2]. The difference of S and non-S types is the degree (S parameter) of orientation of polystyrene chains, the core material of Kuraray's fibers. A modulation of diffractive index is sizable when orientation is well aligned, thus the attenuation length of S type fibers can be shorter. In our previous report [3] we have verified that Kuraray S type fibers are durable against bending at a bending radius as small as ~1 cm. In fiber tracker systems the bending radius of clear fibers could be designed to be somewhat larger. For the purpose of optimizing the S value, we measured the attenuation length and mechanical durability of clear fibers with various S values. In Kuraray's notation, S25 is the standard (non-S) type and S70 is the S type fibers.

The present R&D work has been carried out to design an fiber tracking system IFT [4] in the intermediate region of the CDF upgrade detector at the Fermilab Tevatron. The IFT consists of a set of cylindrical layers of 3HF scintillating fibers of 2 to 3 m length and covers the radial region from 20 cm to 40 cm around the beam pipe. The scintillating light is extracted outside the tracking volume through approximately 6 m long clear fibers. The expected radiation level to 3HF fibers can be estimated by extrapolating the radial dose profile measured with the CDF SVX' located in the range $3 < r < 8$ cm [5]. Extrapolating the dose profile to $r = 20$ (40) cm gives a radiation level of 12 (3.6) krad per integrated luminosity of 1 fb^{-1}. The annual luminosity of the upgraded Tevatron will be 1 fb^{-1} at beginning and 3 fb^{-1} in later years.

The fibers used in the radiation hardness tests were Kuraray multiclad [6] S-type fibers. The diameter was 0.5 – 0.75 mm for 3HF (1% P-TP and 1500 ppm 3HF) fibers and 0.8 mm for clear fibers. The irradiation was performed at the ^{60}Co irradiation facility of Japan Atomic Energy Research Institute (JAERI), Tokai. Section 2 describes the procedure of irradiation and methods of radiation hardness evaluation. The results of the radiation hardness and its parameterization are given in Section 3. In Section 4 we describe the attenuation and mechanical durability of clear fibers as a function of the S parameter. We measured the long term stability of the attenuation of S and non-S type clear fibers, which is also given in Section 4. The results are summarized in Section 5.

2. Irradiation and Evaluation of the Radiation Hardness

2.1 3HF fibers

We have irradiated sample fibers at the JAERI ^{60}Co γ-ray irradiation facility. A cylindrical source container of 9 cm radius is transported in the irradiation cave and placed on an exposure table of ~80 cm in radius. The γ-ray intensity, calibrated with an ion chamber, is nearly proportional to $1/r^2$ and is 4.0 kR/h at a distance of 70 cm for a source of 5.9 kCi intensity. Thus, we can irradiate sample fibers uniformly by setting them at a certain radius around the source. The γ-ray intensity and uniformity were also measured with RCD dosimeter films [7] in the dose range ~10 krad and above, which is the usable range of the RCD films. These two measurements agreed with each other within 10%.

The sample 3HF fibers were 3 m long and wrapped in aluminum foil at irradiation. The ^{60}Co irradiation took place twice for two different sets of samples. In the first irradiation 3HF fibers were placed at fixed distance of 30 cm. These samples had a section near the fiber end shielded with 10-cm thick lead blocks. By measuring the light output continuity along the fiber we investigated the radiation damage to the 3HF wavelength shifter. In the second irradiation we set the samples at three radii 12, 35, and 75 cm, and adjusted the exposure time so that the dose ranges at different radii overlapped each other. Using the overlapped data samples, we investigated the possible dose rate dependence and the mechanical damage due to different fiber curvatures at exposure.

The attenuation curve of 3HF fibers was measured by UV lamp scan with a system shown in Fig. 1. The sample fiber was strung by holding the ends, and a pencil type UV lamp was moved along it using a stepping motor. A through hole was made in the UV lamp enclosure to guide and position the fiber precisely. The illumination spot of $\sim$5 mmϕ was determined by the collimator also machined in the enclosure. The light emerging from the sample 3HF fiber was transmitted through a 3 m long clear fiber of 0.8 mm diameter to a red-sensitive photomultiplier tube, Hamamatsu R2257. The quantum efficiency of this phototube is fairly flat in the entire 3HF emission region, 9% at 500 nm and 8% at 650 nm. The shape of the emission spectrum could change by radiation damage due to wavelength dependence of the transmission degradation, see Section 3.3, use of a flat response PMT is essential in this measurement. The induced current was read out with a picoammeter, Keithley 485. The scanning and data taking were computer controlled.

The UV lamp has an emission spectrum peaking at 360 nm, which can excite the 3HF wavelength shifter but barely the primary flour P-TP. In order to evaluate the radiation damage to P-TP, we also irradiated four 3HF fiber ribbons, each consisting of staggered doublet layers of 16 of 0.5 mmϕ fibers arranged at a 0.6 mm pitch (see Fig. 2), and the light yield was measured by β source scan along the ribbon. Fig. 2 shows a cross sectional view of a sample ribbon and a trigger system for ^{90}Sr β-rays. A ^{90}Sr source set above the sample and a trigger counter set underneath were moved together by a stepping motor. The light yield out of the ribbon was read out with a red-sensitive PMT through a 5-m long clear fiber ribbon. The charge induced by penetrating β rays was measured with an CAMAC ADC. The light yields extrapolated to zero 3HF fiber length is sensitive to the damage to the scintillating processes where both the primary (P-TP) and secondary (3HF) fluors are involved, since the effect from the attenuation degradation can be ignored. These samples were irradiated at a distance of 70 cm from the ^{60}Co source. One out of the four samples had its unread end mirrored with aluminum sputtering. The other samples had the unread end polished.

2.2 Clear fibers

We evaluated the attenuation length of clear fibers by two methods for two different dose ranges. In the higher dose range ($>$ 10 krad), we measured with a PMT the emerging light from the fiber end when 3HF light is injected from the other end of the clear fiber. For this measurement we used a Hamamatsu GaAs PMT R943-02, which had a quantum efficiency from 15% to 12% in the 3HF emission range. The clear fiber length, 5–6 m at the beginning, was shortened successively and this cut and measurement was repeated. Since the radiation hardness of clear fibers is dependent on the wavelength to be transmitted, we used a 3HF scintillating fiber excited by a UV lamp. In order to simulate the case where a charged particle traverses the middle of the IFT, the length between the illuminated point of the 3HF fiber and its end that couples to the clear fiber was set to 1 m. The coupling between the 3HF and clear fibers was provided with a connector, which was not touched during the measurement. We shortened the clear fiber by 50 cm each time at the other end which coupled to the PMT. The cut end was polished with abrasive sheet set on a turning table. The light yield as a function of the clear fiber length can be expressed well by an exponential function, from which we extracted the attenuation length.

Since the accuracy of the attenuation length measurement with the above method was limited by the reproducibility of the fiber end preparation each time in shortening the clear fiber length, we carried out another test to cover the smaller dose range ($<$2 krad) with a setup shown in Fig. 3.

In this test the change of the light output was measured concurrently with ^{60}Co exposure, where we extracted the change of the attenuation length. We used a 0.8 mmϕ clear fiber of 5 m length, to which a 5 cm long 3HF fiber was connected. The 3HF fiber was illuminated by a UV lamp and the induced light was transmitted through the clear fiber to a PMT located outside the irradiation cave. Only a clear fiber section of 2 m length was exposed to ^{60}Co while the remaining part was shielded by lead blocks and the wall of the irradiation cave. The system of the 3HF fiber and the UV lamp was also shielded. The radiation damage to 3HF fibers is caused only through degradation in their attenuation length, as described in the next section. Therefore, even if the radiation to 3HF was not completely eliminated, we can ignore the damage to the 3HF light output by use of such a short 3HF fiber. The stability of the UV lamp and 3HF light source was monitored using a quartz fiber.

3. Results of the Radiation Hardness

3.1 Evaluation of the dose

In γ-ray exposure the energy is deposited mainly by Compton electrons created by ^{60}Co γ's of $\sim$1.2 MeV. Since some fraction of Compton electrons can escape from the sample fiber due to its finite volume, the dose is dependent on the geometry of the sample. The translation factor from Roentgen, given as a function of the distance from the source and the exposure time, to the absorbed dose was calculated using a GEANT simulation. In order to check the reliability of the simulation, we exposed scintillating fiber ribbons of different thicknesses, 0.5, 0.75, and 1.5 mmϕ, to a ^{60}Co source, and measured the induced current. The measured ratio of the current normalized by volume out of the 0.5 mmϕ fiber ribbon to that out of the 1.5 mmϕ fiber ribbon was 0.85$\pm$0.04, while we obtained a simulated ratio of 0.80$\pm$0.03. The simulation can provide results consistent with the experimental results. The Roentgen-to-dose translation factor for single fibers was extracted from simulation. With use of Al foils as the wrapping material, the translation factor is made almost constant within 0.6 to 0.7 for fibers of diameter smaller than 1 mm. We hereafter take a translation factor of 0.65 for single fibers. The overall uncertainty of the dose is about 20%.

3.2 Radiation hardness of 3HF fibers

Fig. 4 shows an example of the 3HF attenuation curves measured as a function of the UV lamp position, x. The fiber was irradiated to 48 krad at 12 krad/h uniformly along the fiber except the part $x < 45$ cm, which was shielded by lead blocks. The light yields are normalized by the average of the three data points at $x = 20$, 30 and 40 cm. The four curves in the figure are those measured before, 2 days after, 13 days after and 260 days after the irradiation. Since no discontinuity is visible for the irradiated sample across the position $x = 45$ cm, we conclude that 3HF scintillation mechanism itself is not destroyed up to this dose. Instead, the attenuation length is shortened; fitting the curves in $x > 50$ cm gives the attenuation length 4.5 m and 2.45 m before and 13 days after the irradiation, respectively. The attenuation length gradually recovered as is evident from the figure, which will be discussed in Section 3.4.

Measurements of doublet fiber ribbons using penetrating β-rays are summarized in Table 1. The damage to the light yield is small at positions close to $x = 0$ as shown in the table. Extrapolations to $x = 0$ are consistent with no damage within the measurement uncertainty for the samples with no mirror. The sample with mirror showed some deviation from unity, which is due to that the light component reflected by the mirror is reduced by the attenuation length degradation. The present results support the previously obtained conclusion [8] that both of the scintillating dyes P-TP and 3HF are not damaged in the dose range under study.

In Fig. 5 we plot the ratios of the attenuation lengths after to before the irradiation for 3HF fibers and 3HF fiber ribbons. The measurements were made 1–2 weeks after the irradiation. Also plotted are results for clear fibers, which are described in the following section.

We expect that damage to 3HF fibers and to clear fibers are similar if the damage is expressed by the ratio of the attenuation lengths before to after irradiation, since the damage to both fibers occurs through degradation in the attenuation length. In fact, the data points in Fig. 5 seem to lie on a single line:

$$\lambda/\lambda_0 = (0.80 \pm 0.01) - (0.144 \pm 0.007) \log_{10} D : D > 0.1\text{krad} \tag{1}$$

where D is the dose in krad and λ_0 is the attenuation length with no damage.

We note that the 3HF fiber samples exposed at different distances from the ^{60}Co source, 12 cm to 75 cm, do not significantly deviate from each others. Therefore we expect there should be no significant improvement in the radiation hardness when fibers are kept straight at irradiation, which is relevant for fibers used in trackers.

3.3 Radiation hardness of clear fibers

Radiation hardness of clear fibers, plotted in Fig. 5, is similar to that of 3HF fibers as far as the ratio of the attenuation lengths after to before the irradiation is compared. In Fig. 5 the drop of the clear fiber attenuation length measured concurrently with the irradiation is also shown by the shaded region. This sample was irradiated at a rate of 2 krad/h. Assuming an exponential attenuation in the clear fiber, one can extract the ratio of the attenuation lengths during to before the irradiation through the relation:

$$\lambda/\lambda_0 = (\frac{\lambda_0}{l_0} \ln \frac{L_0}{L} + 1)^{-1}, \tag{2}$$

where λ/λ_0 is the ratio of the attenuation lengths during to before irradiation, l_0 is the length of exposed part (2 m), and L/L_0 is the ratio of the light outputs. From the measurement of L/L_0, the ratio of the attenuation lengths can be calculated. We measured the attenuation lengths of the irradiated and shielded sections separately after the irradiation. We obtained $\lambda_0 = 6.6$ m for the shielded section, which is taken in the calculation. The shaded region corresponds to the systematic uncertainties. Among these the contribution from the instability of the 3HF light source (the UV lamp instability and the 3HF damage induced by the UV lamp and irradiation) was evaluated to be at most 5% where the main cause of the instability was the temperature variation. We recognized that the output current changed by 2–3% in a minute right after the source was removed. The systematic uncertainties include also this short time light output variation and the uncertainty in λ_0.

As described before we used a 3HF scintillating fiber as light source for attenuation measurements of clear fibers, since the absorption is dependent on the wavelength of the light to be transmitted. Fig. 6 shows the absorption spectra of a unirradiated and two irradiated samples. The irradiated samples were measured eight days after the irradiation. The absorption was measured with an optical spectrum analyzer, Anritsu MS9701, and was defined as the ratio of the light yield from a 6 m clear fiber and that from a 1 m fiber. The attenuation length λ is thus related to the absorption A through

$$\lambda[\mathrm{m}] = 5[\mathrm{m}]/\ln(10^{\frac{A}{10}}) = 21.7[\mathrm{m}]/A. \tag{3}$$

Hence, $\lambda = 10.8$ (5.4) m for $A = 2$ (4) dB/5m. Larger absorption in shorter wavelengths is due to Rayleigh scattering. The peaks in the spectrum are characteristic absorption bands of polystyrene molecule. The damage to the attenuation length is larger at shorter wavelengths and is negligibly small at wavelengths longer than 700 nm. Note that the 3HF emission spectrum ranges from 500 nm to 650 nm with the peak at 530 nm.

3.4 Recovery of the radiation damage

The expected dose rate in the IFT is at most $\sim$2 rad/h, while we irradiated the samples at accelerated rates of 2–60 krad/h. Ref. 1 reports that the attenuation length of 3HF fibers irradiated to 140 krad at 16 krad/h showed a drop substantially (to 20% or less of the original length) right after the irradiation but recovered to $\sim$50% in $\sim$10 h. The recovery was traced for a couple of days, and seems to be stable in this period. Another group [9] has studied the recovery of the attenuation length of fibers exposed to ambient fluorescence light and reports that the damage is recovered completely in 5–20 days. The radiation damage is explained by creation of free radicals, which act as color centers and degrade the light transmission. The recovery is the process where oxygen reacts with such free radicals yielding oxidation products or thermal annealing is taking place [8]. The radiation-induced coloration thus starts to disappear after irradiation and the transmittance is recovered, but such oxidation products can degrade the transmittance [8], which is one of the causes for the permanent damage in the attenuation length.

Fig. 7 plots the recovery of the attenuation length of 3HF fibers measured in the period up to 260 days after the irradiation. The samples were kept in the air at room temperature and shielded against ambient light. Although the damage measured 3 days after the irradiation is dependent on the accumulated dose, the recovery seems to occur similarly for the doses we tested. Also the recovery rate seems similar for the two dose rates 2 and 12 krad/h we measured. The ratio of the attenuation length can be expressed approximately by

$$\lambda(\mathrm{T})/\lambda_0 = a_0 + (9-12)\% \log_{10}(\mathrm{T}) : \mathrm{T} > 3 \tag{4}$$

where a_0 is the ratio measured 3 days after the irradiation and T is in days.

Such a slow recovery is also reported in [10]. In Ref. 10, 3HF and clear fibers (Kuraray multiclad fibers) were irradiated by a ^{137}Cs source at $\sim$20 krad/h to 0.5 Mrad. The light yield out of 1 m long 3HF fibers was $\sim$20% of the original light yield just after irradiation, $\sim$20% after 20 days and 55–90% (varies between samples) after two months, while the light output out of clear fibers was nearly constant at 30–50% during the same period. By assuming an exponential attenuation in 3HF fibers and $\lambda_0 \sim$3 m, the initial damage of 20% of the original light yield can be translated into degradation in the attenuation length of $\lambda/\lambda_0 \sim$0.17, which should be compared with our ratio of $\sim$0.4 at 0.5 Mrad. Although the magnitude of the initial damage seems not identical, the tendency of the recovery is roughly consistent with each other. We have no data available for clear fibers, because of our destructive tests and we did not keep extra fibers.

Because of existence of a slow recovery component, evaluation of the detector performance in the real radiation environment is not straightforward. We have carried out a GEANT simulation to evaluate the dose profile along the 3HF and clear fibers of the IFT. Using the damage parameterization Eq. (1), the light yield is calculated to decrease by 38–35% (48–45%) of the original light yield after a delivered luminosity of 3 (10) fb^{-1}, where the range of the numbers corresponds to the different position of the 3H fibers from the beam pipe. Of these drops about 1/4 is due to the clear fiber and the rest is due to the 3HF fiber. The actual damage during the experiment may have to be evaluated through irradiation tests at much lower dose rates where the recovery process should be taking place concurrently with damaging process. Here we evaluate the impact of a year long break of operation scheduled after 3 fb^{-1}. The light yield decreases by 38–35% if we assume no recovery during the experiment, as mentioned above. This drop will recover according to Eq. (4), resulting a smaller drop of 21–14% if only 3HF is assumed to recover.

4. Durability of the clear fibers

4.1 Attenuation length dependence on the S parameter

The S parameter is a characteristic index of the degree of orientation of polystyrene chains along the fiber axis. At larger S values polystyrene chains are aligned and the fibers can become softer and more flexible. On the other hand, the attenuation length can be shorter due to possible modulation of diffractive index values along the fiber. An extreme case of larger S values would be the fishing string which is strong and flexible but is not transparent.

We have changed the parameter S from S25 (non-S type) to S70 (S type) and measured the attenuation length. A set of sample fibers were fabricated from the same preform, therefore we can ignore the individual difference otherwise arising due to different preform. Fig. 8 shows the attenuation lengths as a function of the S parameter, the attenuation length being measured for 1–4 samples at each S value. The attenuation length decreases with S. For example, the attenuation length of S40 is typically 12 m, while that of S70 is 9 m. Since S40 is substantially superior over S25 and S30 in view of mechanical durability as described below, we have carried out another comparison measurement between S40 and S70 where we measured the emerging light yield when 3HF light was injected from the other end of 6 m long samples. From the average of 10 samples each for S40 and S70, the light yield out of S40 fibers was larger by 16% than that out of S70 fibers, which is consistent with the improvement expected from the longer attenuation length of S40 fibers.

4.2 Transmittance degradation at bending

In order to qualify the mechanical durability against bending, we measured the transmittance of sample clear fibers rolled around plastic tubes of 0.5, 1 and 2 cm in radius. The number of turns were 20, 16 and 16, respectively. In this measurement the samples were coupled to green LEDs and the emerging light yields were measured by a common PMT. By switching the LEDs the transmittance of the corresponding fiber was traced for over two months. The possible variation of the LED intensity was monitored by another PMT.

Fig. 9 plots the stability of the light output for fibers rolled at radii of 1 and 2 cm. The data are shown only for S25 (non-S), S30 and S40, since S50–S70 showed stable light output similar to S40. The light output of S25 started to drop in an hour and went down to almost zero in a day, while that of S40 was stable during this period of measurement. At a bending radius of 0.5 cm, the fibers S40 through S60 also showed a substantial drop just after they were rolled, although the tendency that the fibers are more flexible for larger S values is still valid. From these measurements we conclude that S40 is substantially durable against bending in comparison with S30 and S25 as long as the bending radius is kept larger than $\sim$1 cm.

4.3 Long term stability of clear fiber attenuation length

The long term stability of the clear fiber transmittance is an interesting issue to pursuit for long term stability point of view of the detector performance. It is also important for the way of storing the fiber whether the fiber has to be kept straight or can be reeled. We measured periodically the attenuation length for almost three years both for S and non-S type fibers of 0.8 mmϕ thickness. The fibers have been rolled on reels of 50 cm in radius since the production. The reels have been contained in a wooden box, which has been kept in our laboratory at room temperature. Although the fibers have never been exposed to intense light such as direct rays of the sun, the fibers were exposed to ambient room light in the period for ~200 days after production where the lid of the wooden box was open: after that the fibers were kept in dark.

The results are plotted in Fig. 10. The number of samples was typically two for each of S and non-S type fibers. The attenuation length is fairly stable in this period of three years since production. The attenuation length may slightly decrease from that right after the production, which could be attributed to effect of ambient room light described above or to any other initial effect that shortens the attenuation length of new fibers. The attenuation lengths are approximately 12 m and 8 m for non-S and S type fibers even after three years.

5. Summary

We have measured the radiation hardness of Kuraray 3HF scintillating and clear fibers in the dose range from ~0.4 krad to 0.5 Mrad, and studied the optical and mechanical properties of clear fibers with various S values. The ratio of the attenuation lengths before and after the irradiation is similar for the both 3HF and clear fibers. The damage function derived from the data measured 1–2 weeks after the irradiation is given in this note. The damage of 3HF fibers showed a substantial recovery with a time scale of a few months. The recovery rate is rather insensitive to the dose rate 2–12 krad/h and to the accumulated dose of 6–48 krad we tested. We have shown that the attenuation length of clear fibers is longer for smaller S values. For a bending radius of >1 cm, S40 seems to be a good compromise, which is mechanically durable and the attenuation length is longer by ~30% than S-type (S70) fibers. The attenuation length of clear fibers which have been reeled at a radius of 50 cm was traced for three years. The attenuation length turned out to be fairly stable in this period.

Acknowledgments

We would like to thank O. Shinji (Kuraray) for preparing the sample fibers and H. Nagayama (JAERI) for carrying out ^{60}Co irradiation. This work was supported by the Japanese-US cooperation in the field of High Energy Physics.

References

[1] S. Margulies et al., Proc. SCFI93 Workshop on Scintillating Fiber Detectors, Notre Dame, edited by A.D. Bross, R.C. Ruchti and M.R. Wayne, World Scientific (1995) 421.

[2] See, for example, CDF Plug Upgrade Tile/Fiber Calorimeter, The CDF II Detector Technical Design Report, FERMILAB-Pub-96/390-E (1996).

[3] K. Hara et al., Nucl. Instr. and Meth. A373 (1996) 347.

[4] Proposal for RUN II Tracking System Upgrades for CDF, CDF/TRACKING/PUBLIC/3079 (1995). This fiber system, however, was not adopted as the intermediate tracking device for CDF.

[5] D. Amidei et al., Nucl. Instr. Methods, A 350, 73 (1994); P. Azzi et al., CDFnote 3278. The dose measured with a dosimeter was 300 rad/pb^{-1} for the SVX layer 0 (r = 3 cm). The radial dependence $r^{-1.7}$ was obtained from the increases in the leakage current measured for the layers 0 to 3 ($3 < r < 8$ cm).

[6] Multiclad fibers have two cladding layers of PMMA (n=1.49) and fluorinated MMA (n=1.42) surrounding a polystyrene core (n=1.59). Existence of the second clad makes high the light trapping efficiency. See S. Aota et al., Nucl. Instr. and Meth. A357 (1995) 71.

[7] Far West Technologies, Goleta, CA. USA.

[8] See, for example, A. D. Bross and A. Pla-Dalmau, Nucl. Instr. and Meth. A327 (1993) 337; A. D. Bross and A. Pla-Dalmau, IEEE Trans. Nucl. Sci. 39 (1992) 1199

[9] M. Chung and S. Margulies, Proc. SCFI93 Workshop on Scintillating Fiber Detectors, Notre Dame, edited by A.D. Bross, R.C. Ruchti and M.R. Wayne, World Scientific (1995) 431.

[10] F. Bedeschi et al., CDF note 3583.

Table 1: Ratio of the light yields and the attenuation lengths after to before the irradiation, measured for 3HF ribbons. One of the four samples has aluminum mirror at the unread fiber ends.

	47krad	380krad		680krad
	w/o mirror	w/o mirror	w/ mirror	w/o mirror
light yield ratio at 0.1 m	0.97 ± 0.07	0.96 ± 0.04	0.86 ± 0.08	0.95 ± 0.05
light yield ratio at 1.1 m	0.88 ± 0.07	0.70 ± 0.03	0.69 ± 0.07	0.67 ± 0.03
light yield ratio at 2.1 m	0.77 ± 0.06	0.64 ± 0.02	0.63 ± 0.04	0.53 ± 0.02
attenuation length ratio	0.73 ± 0.07	0.59 ± 0.03	0.43 ± 0.08	0.40 ± 0.02

Figure Captions

Fig. 1. Setup used to measure the attenuation length of 3HF fiber.

Fig. 2. Cross sectional view of the light yield measurement system of a 3HF fiber ribbon. Penetrating β-rays are triggered by a scintillator viewed by two PMT's. Soft β-rays are absorbed by a 4 mm thick PMMA plate set underneath the sample 3HF ribbon.

Fig. 3. Setup used to measure the attenuation length change of a clear fiber at irradiation.

Fig. 4. Attenuation curves of a 3HF fiber measured before (open squares), 3 days (triangles) after, 13 days after (crosses), and 260 days after (filled squares) the irradiation. The dose was 48 krad excluding the part from 0 to 45 cm which was shielded by lead blocks.

Fig. 5. Ratio of the attenuation lengths before to after irradiation. The samples are 3HF fibers (open marks), 3HF fiber ribbons (crosses), and clear fibers (filled marks). The fiber curvature at irradiation and the dose rate are given in parentheses. The shaded region shows the range of the ratio for a clear fiber where the attenuation length was evaluated concurrently with irradiation at 2 krad/h (see text). Other data were measured 1–2 weeks after the irradiation.

Fig. 6. Absorption spectra of clear fibers unirradiated, irradiated to 0.2 Mrad, and irradiated to 0.5 Mrad.

Fig. 7. Recovery of the attenuation length of 3HF fibers, irradiated at two different dose rates and to four different doses. Typical size of the systematic uncertainty is indicated for the sample irradiated at 2 krad/h.

Fig. 8. Attenuation length of 0.8 mm ϕ clear fibers as a function of S parameter. The light source is 3HF scintillating fiber excited by a UV lamp. Typical size of measurement uncertainty is indicated for some of the data.

Fig. 9. Light output as a function of elapsed time since fibers were bent. The fibers were rolled by 16 turns at a radius of 1 cm (open marks) and of 2 cm (filled marks).

Fig. 10. Attenuation length of clear fibers as a function of elapsed time since production. The fibers, S and non-S types, were rolled on reels of 0.5 m in radius.

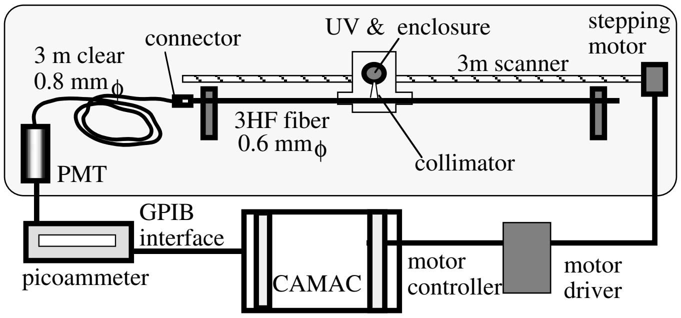

Figure 1: Setup used to measure the attenuation length of 3HF fiber.

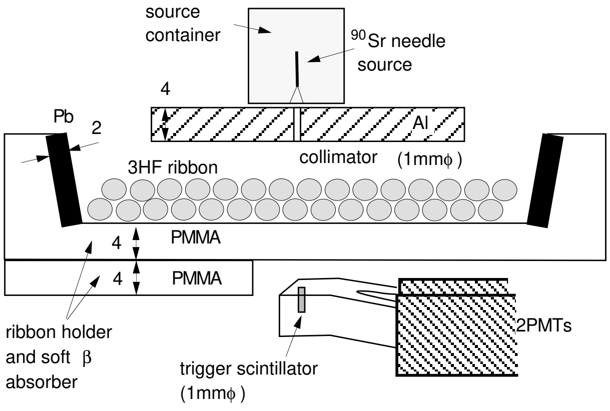

Figure 2: Cross sectional view of the light yield measurement system of a 3HF fiber ribbon. Penetrating β-rays are triggered by a scintillator viewed by two PMT's. Soft β-rays are absorbed by a 4 mm thick PMMA plate set underneath the sample 3HF ribbon.

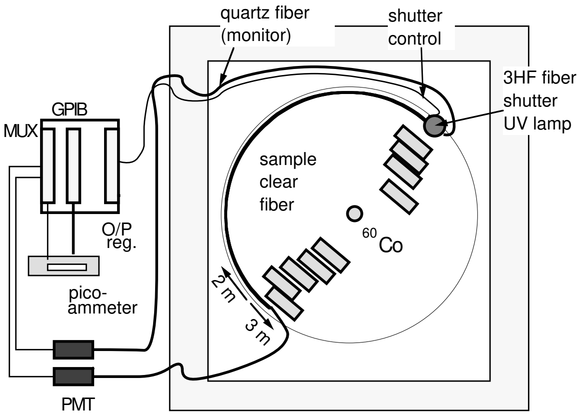

Figure 3: Setup used to measure the attenuation length change of a clear fiber at irradiation.

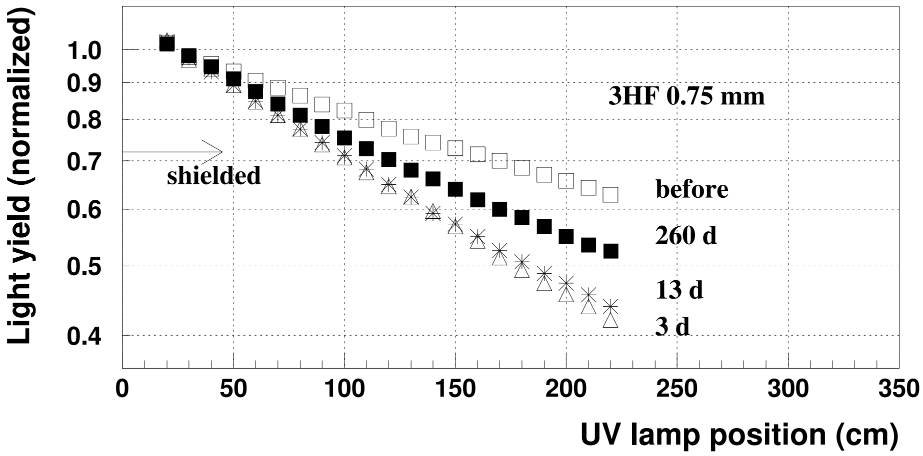

Figure 4: Attenuation curves of a 3HF fiber measured before (open squares), 3 days (triangles) after, 13 days after (crosses), and 260 days after (filled squares) the irradiation. The dose was 48 krad excluding the part from 0 to 45 cm which was shielded by lead blocks.

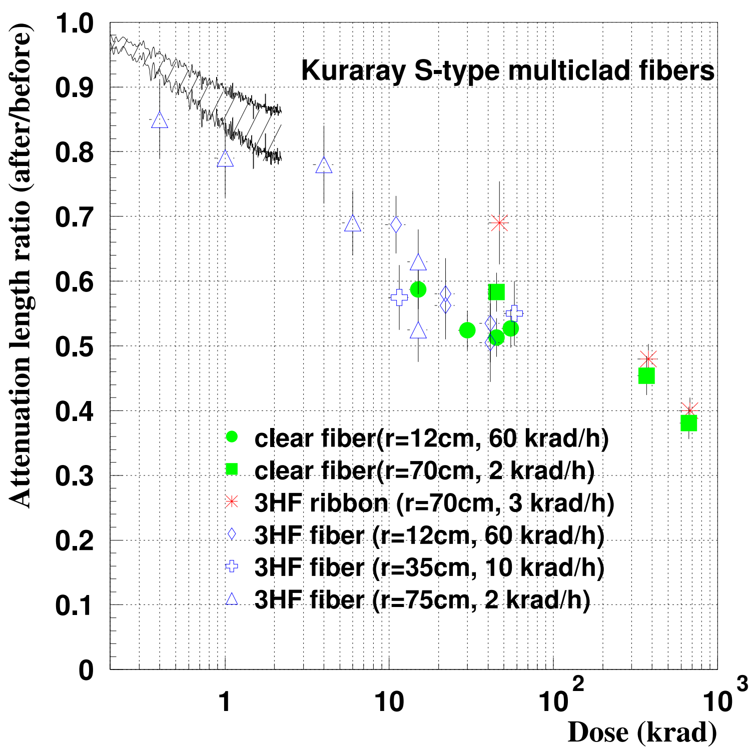

Figure 5: Ratio of the attenuation lengths before to after irradiation. The samples are 3HF fibers (open marks), 3HF fiber ribbons (crosses), and clear fibers (filled marks). The fiber curvature at irradiation and the dose rate are given in parentheses. The shaded region shows the range of the ratio for a clear fiber where the attenuation length was evaluated concurrently with irradiation at 2 krad/h (see text). Other data were measured 1–2 weeks after the irradiation.

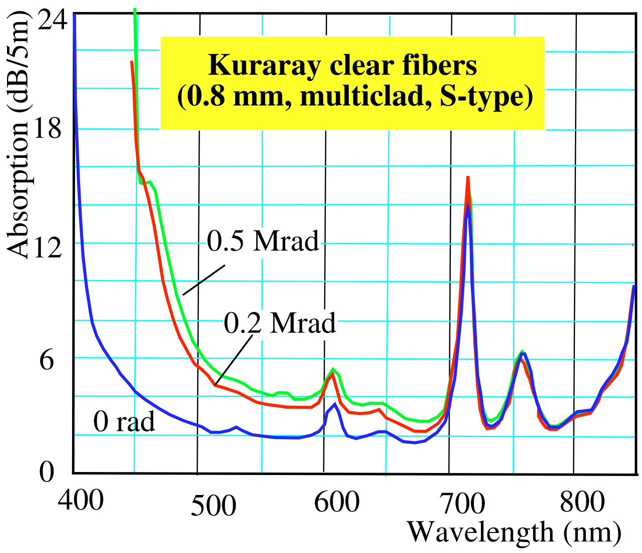

Figure 6: Absorption spectra of clear fibers unirradiated, irradiated to 0.2 Mrad, and irradiated to 0.5 Mrad.

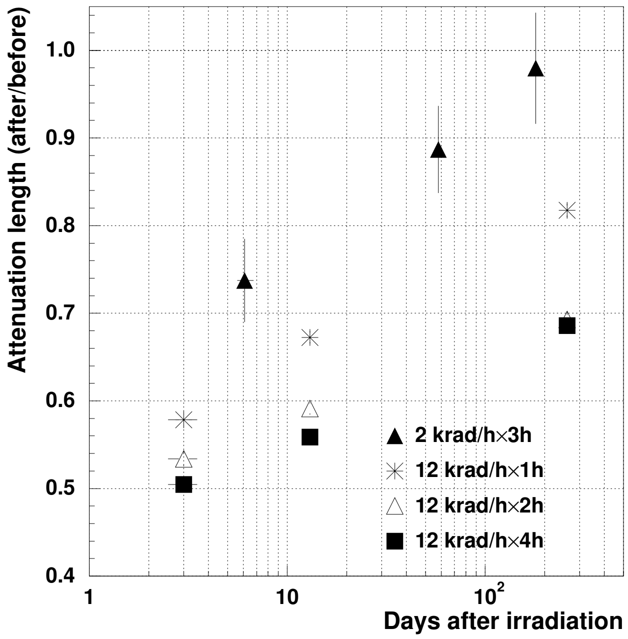

Figure 7: Recovery of the attenuation length of 3HF fibers, irradiated at two different dose rates and to four different doses. Typical size of the systematic uncertainty is indicated for the sample irradiated at 2 krad/h.

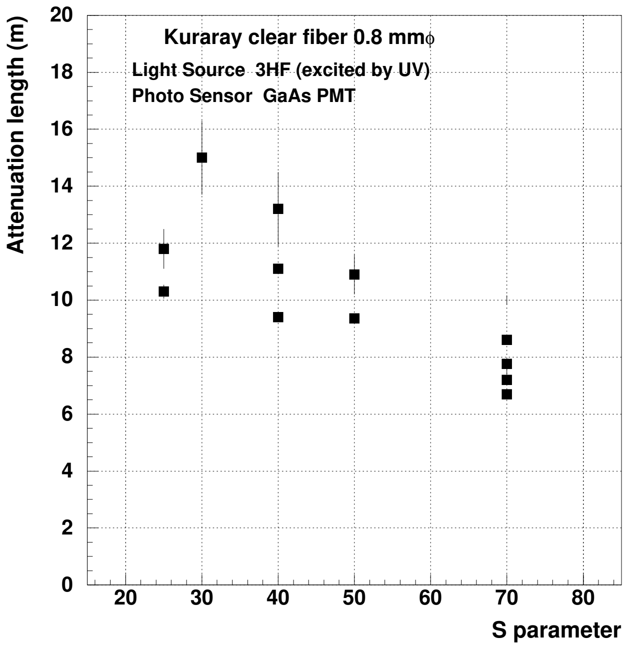

Figure 8: Attenuation length of 0.8 mm ϕ clear fibers as a function of S parameter. The light source is 3HF scintillating fiber excited by a UV lamp. Typical size of measurement uncertainty is indicated for some of the data.

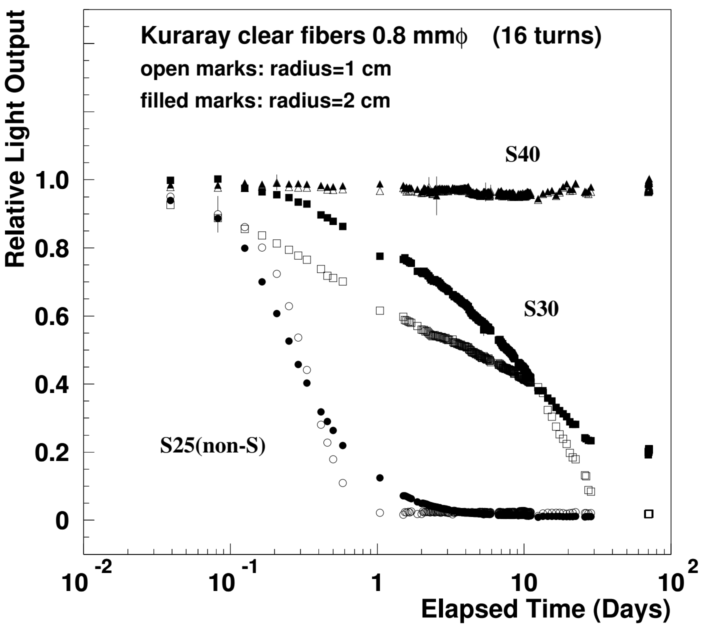

Figure 9: Light output as a function of elapsed time since fibers were bent. The fibers were rolled by 16 turns at a radius of 1 cm (open marks) and of 2 cm (filled marks).

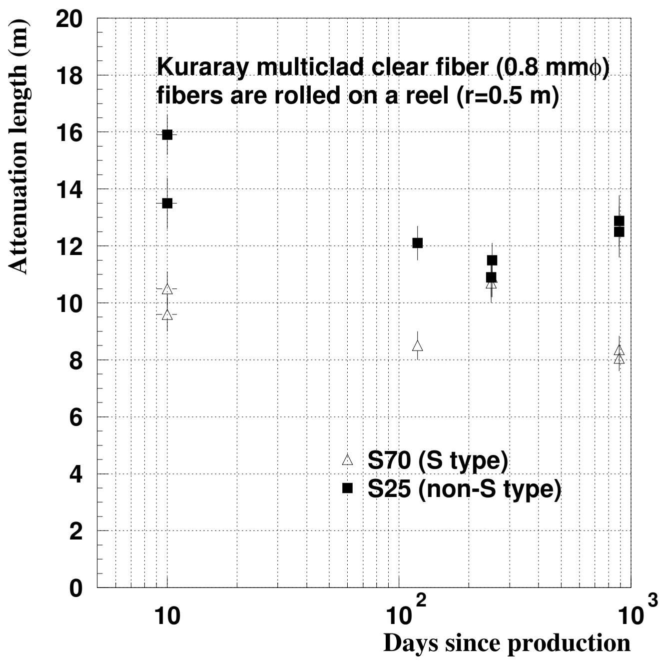

Figure 10: Attenuation length of clear fibers as a function of elapsed time since production. The fibers, S and non-S types, were rolled on reels of 0.5 m in radius.